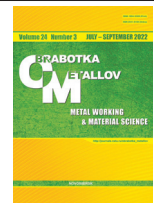




# Obrabotka metallov -

# Metal Working and Material Science

Journal homepage: [http://journals.nstu.ru/obrabotka\\_metallov](http://journals.nstu.ru/obrabotka_metallov)



## Numerical analysis of the process of electron beam additive deposition with vertical feed of wire material

Gleb Permyakov<sup>1, a, \*</sup>, Roman Davlyatshin<sup>1, b</sup>, Vladimir Belenkiy<sup>1, c</sup>,  
 Dmitry Trushnikov<sup>1, d</sup>, Stepan Varushkin<sup>1, e</sup>, Shengyong Pang<sup>2, f</sup>

<sup>1</sup> Perm National Research Polytechnic University, 29 Komsomolsky Prospekt, Perm, 614990, Russian Federation

<sup>2</sup> Huazhong University of Science and Technology, Luoyu street No1037, Hongshan district, Wuhan city, 430074, China

<sup>a</sup>  <https://orcid.org/0000-0001-8158-3460>,  [gleb.permyakov@yandex.ru](mailto:gleb.permyakov@yandex.ru), <sup>b</sup>  <https://orcid.org/0000-0002-7388-7699>,  [romadavly@gmail.com](mailto:romadavly@gmail.com),

<sup>c</sup>  <https://orcid.org/0000-0001-7869-6632>,  [vladimirbelenkij@yandex.ru](mailto:vladimirbelenkij@yandex.ru), <sup>d</sup>  <https://orcid.org/0000-0001-7105-7934>,  [trdimitr@yandex.ru](mailto:trdimitr@yandex.ru),

<sup>e</sup>  <https://orcid.org/0000-0002-9346-6445>,  [stepan.varushkin@mail.ru](mailto:stepan.varushkin@mail.ru), <sup>f</sup>  <https://orcid.org/0000-0002-5171-4148>,  [spang@mail.hust.edu.cn](mailto:spang@mail.hust.edu.cn)

### ARTICLE INFO

#### Article history:

Received: 19 April 2022

Revised: 28 April 2022

Accepted: 18 June 2022

Available online: 15 September 2022

#### Keywords:

Electron Beam

Electron beam surfacing

Additive technologies

Numerical experiment

#### Funding

This work was financially supported by the Ministry of Education and Science of Perm Krai (Agreement S-26/508 of 09.03.2021) and the Ministry of Science and Higher Education of the Russian Federation (State Task No. FSNM-2021-0011 and No. FSNM-2020-0028).

#### Acknowledgements

Research were partially conducted at core facility “Structure, mechanical and physical properties of materials”.

### ABSTRACT

**Introduction.** At present, additive technologies are actively developing all over the world and are becoming more and more widely used in industrial production. The use of electron beams in additive processes of directed energy input, the so-called Directed Energy Deposition (DED) technologies, has several advantages, the main ones being the flexibility of controlling the spatial and energy characteristics of the thermal source and the presence of a vacuum protective environment. The standard scheme for additive electron beam deposition is melting of a wire filler material fed from the side into the electron beam affected area, but this additive electron beam deposition pattern does not provide a uniform thermal impact in the deposited area. The most effective method for electron-beam deposition is vertical wire feeding, which provides the most stable formation of the liquid metal bath and, consequently, the deposited beads. At the same time, so far there are no results of numerical analysis of this process in order to determine its main regularities. **The aim of the work** is to carry out numerical experiments for qualitative analysis and determination of the regularities of formation of deposited beads and transfer of filler material, the dependence of the geometric characteristics of the obtained beads on the influence of vapor pressure forces, direction and value of the azimuthal angle of heat sources. **The research methods** were a series of numerical experiments, which analyzed variants of the electron-beam surfacing process at the location of the surfacing rate vector in the action plane of electron beams and perpendicular to this plane to determine the basic regularities of deposited beads formation and transfer of filler material, dependence of geometric characteristics of obtained beads on the influence of vapor pressure forces, direction of heat sources and the azimuth angle of heat sources. **Results and discussion.** It is found that the geometric characteristics of the deposited beads significantly depend on the relative position of the deposition velocity vector with respect to the plane of the electron beams, and consideration of the vapor pressure has a significant influence on the results of numerical simulation of the weld pool formation and the hydrodynamic processes occurring in it. In this case, the location of the deposition velocity vector perpendicular to the action plane of the electron beams, there is a more uniform geometry of the deposited metal beads, and increasing the azimuthal angle of the heat sources increases the probability of spitting to the periphery of the deposited bead, which is associated with limitation of the melt motion in the longitudinal direction by the vapor pressure forces.

**For citation:** Permyakov G.L., Davlyatshin R.P., Belenkiy V.Y., Trushnikov D.N., Varushkin S.V., Pang S. Numerical analysis of the process of electron beam additive deposition with vertical feed of wire material. *Obrabotka metallov (tehnologiya, oborudovanie, instrumenty) = Metal Working and Material Science*, 2022, vol. 24, no. 3, pp. 6–21. DOI: 10.17212/1994-6309-2022-24.3-6-21. (In Russian).

#### \* Corresponding author

Permyakov Gleb L., Ph.D. (Engineering), Researcher,

Perm National Research Polytechnic University

29 Komsomolsky Prospekt,

614990, Perm, Russia

Tel.: +7 (964) 18504-75, e-mail: [gleb.permyakov@yandex.ru](mailto:gleb.permyakov@yandex.ru)

## Introduction

Nowadays additive technologies are actively developing all over the world and are increasingly being used in industrial production. The overall growth of the additive technology market is more than 20 % annually. Additive manufacturing is based on a new efficient concept of digital production, in which there is a close link between all stages of product design and production, ensured by the presence of a digital prototype of the product and the application of end-to-end design principles.

Powders or wire materials are used for printing metal components. The use of powders makes it possible to obtain the final product with complex geometry and high surface quality, but the application of these technologies is constrained by the high cost of powder materials and low productivity. The use of wire as a starting material allows achieving high process productivity and a significant economy compared to powder technology due to the use of a cheaper wire material.

The use of electron beam in the additive processes of directed energy input, the so-called *Directed Energy Deposition (DED)* technologies, has several advantages, the main among which are the flexibility of controlling the spatial and energy characteristics of the thermal source and the availability of a vacuum protective medium [1–5]. Such technologies began to be actively used in industry since the early 2000s for the production of jet engine parts, turbine blades and other items made of structural steel and nonferrous alloys [5–10]. The combination of these technologies with subsequent machining allows achieving high part production efficiency compared to traditional technologies.

The product manufacturing stage is preceded by preliminary simulation in order to determine the parameters of the product manufacturing technology to ensure the required performance characteristics. At the same time, the reliability of simulation results largely depends on the quality and adequacy of the process model used. The possibility of simulation of the technological process is of high interest and is a reserve for optimizing the technological modes of parts manufacturing, developing control programs, minimizing defects and improving the quality of manufacturing of complex parts.

One important factor in electron-beam additive technology processes that use wire deposition is the wire feed orientation.

The standard scheme for additive electron-beam deposition is the electron-beam melting of a wire filler material fed laterally into the electron-beam zone. This additive electron-beam deposition scheme does not provide uniform thermal influence in the deposited area because the electron beam does not interact with part of the deposited surface as a result of its shading by the filler wire. A number of models of this process have been developed dedicated to the analysis of heat and mass transfer processes during additive shaping [11–14].

The most effective variant for electron-beam deposition is vertical wire feeding, which provides the most stable formation of the welding pool and, accordingly, the deposited beads. In this case, to melt vertically fed wire, it is advisable to use two electron beam guns that melt the filler wire symmetrically. In work [15] a mathematical model of the melting process of vertically fed wire material by two symmetrically arranged electron beams without taking into account the vapor pressure forces, as well as additional process parameters, such as the location and angle of the heat sources, which has a significant impact on the results of numerical simulation of the welding pool formation and the hydrodynamic processes occurring in it.

In accordance with this, the purpose of this work was to conduct numerical experiments for qualitative analysis and determination of the basic regularities of formation of deposited beads, the modes of filler material transfer and the dependence of geometric characteristics of the deposited beads on the influence of the vapor pressure forces, the relative position of the deposition vector and the plane of electron beams and the value of the azimuth angle of the heat sources.

## Research methods

During additive electron-beam deposition with two symmetrically acting electron beams in the process of substrate motion, different variants of the location of the plane in which the electron beams act, relative to the deposition rate vector and the value of the azimuthal angle of the heat sources are possible.

In this work, the numerical simulation used the mathematical model previously developed by the authors [15], which considers the interaction of solid and liquid metal. There are two phases for this:  $\Omega^l$  – liquid and  $\Omega^s$  – solid, the combination of which represents the entire study area –  $\Omega$ . The solid phase, in turn, consists of a wire  $\Omega^{wire}$  and substrate  $\Omega^{sub}$ . The motion of a metallic melt can be described as the motion of a viscous incompressible fluid. In the general case, the system of equations will consist of differential equations describing the evolution of density  $\rho$ , velocities  $\mathbf{u}$  and temperature  $T$  in the form of balance laws (mass, momentum, and energy balance equations, respectively):

$$\begin{cases} \frac{d\rho}{dt} = -\rho \nabla \cdot \mathbf{u}, & \mathbf{R} \in \Omega^{wire}, \\ \frac{d\mathbf{u}}{dt} = \frac{1}{\rho} (-\nabla p + \mathbf{f}_v + \mathbf{f}_s + \mathbf{f}_v) + \mathbf{g}, & \mathbf{R} \in \Omega^l, \\ \frac{d\rho}{dt} = 0, \quad \frac{d\mathbf{u}}{dt} = 0, & \mathbf{R} \in \Omega^s, \\ \rho c_p \frac{dT}{dt} = -\nabla \cdot \mathbf{q} - s_v - s_{rad}, & \mathbf{R} \in \Omega, \end{cases} \quad (1)$$

where  $\mathbf{u}$  is velocity,  $\rho$  is density,  $\mathbf{f}_v$  is viscous forces,  $\mathbf{f}_s$  is surface tension force,  $\mathbf{f}_v$  is vapor pressure force,  $\mathbf{g}$  is acceleration of gravity,  $c_p$  is specific heat,  $\mathbf{q}$  is heat flux,  $k$  is heat transfer coefficient,  $s_v$  is evaporation heat loss,  $s_{rad}$  is heat loss due to radiation.

Density  $\rho$  and pressure  $P$  are related by means of the equation of state:

$$P(\rho) = \frac{c_0^2 \rho_0}{7} \left[ \left( \frac{\rho}{\rho_0} \right)^7 - 1 \right], \quad (2)$$

where  $c_0$  and  $\rho_0$  are sound propagation velocity and density at zero applied tension, respectively.

For incompressible fluids, the viscous forces will take the following form:

$$\mathbf{f}_v = \eta \nabla^2 \mathbf{u}, \quad (3)$$

where  $\eta$  is dynamic viscosity.

Following the continuum approach of *Brackbill* and *Cote* [16], based on *Continuous Surface Force (CSF)*, the surface tension effects are treated as volume forces in equation (1), distributed over an interfacial volume of finite width. The surface tension force is the sum of the normal and tangential components:

$$\mathbf{f}_s = -\alpha k \mathbf{n} + (\mathbf{I} - \mathbf{n}\mathbf{n}) \nabla \alpha, \quad (4)$$

where  $\alpha$  is surface tension coefficient,  $k = \Delta n$  is surface curvature,  $\mathbf{n}$  is surface normal,  $\mathbf{I}$  is unit tensor,  $\nabla \alpha = d\alpha(T)/dT$ . The dependence of the surface tension coefficient on temperature is selected as linear:

$$\alpha(T) = \alpha_0 - \alpha'_0 (T - T_0), \quad (5)$$

where  $\alpha_0$  is surface tension coefficient at temperature  $T_0$ . This dependence describes the Marangoni effect.

In addition to the standard capillary effects, the high temperatures inherent in additive manufacturing processes cause the metal to evaporate, which leads to vapor pressure forces and heat loss due to evaporation. Usually a phenomenological model is used to simulate these processes [17, 18]:

$$\mathbf{f}_v = -p_v(T) \mathbf{n}, \quad p_v(T) = C_p \exp \left[ -C_T \left( \frac{1}{T} - \frac{1}{T_v} \right) \right], \quad (6)$$

where  $T_v$  is boiling point, constants  $C_p = 0.54 p_a$  and  $C_T = h_v/R$  include atmospheric pressure  $p_a$ , molar latent heat of fusion  $h_v$  and molar gas constant  $R$ .

Following the same phenomenological model as for the vapor pressure, the heat loss due to evaporation has the form:

$$S_v = -m_v [h_v + h(T)], m_v = 0.82c_s p_v(T) \sqrt{\frac{C_M}{T}}, h(T) = \int_{T_{h,0}}^T c_p dT, \quad (7)$$

where enthalpy rate per surface unit area  $S_v$  is obtained from the product of vapor mass flow per unit surface area  $m_v$  and the sum of the specific enthalpy  $h(T)$  and the latent heat of vaporization  $h_v$  per unit mass.  $T_{h,0}$  is the initial temperature of the specific enthalpy, and the constant  $C_M = M / (2\pi R)$  contains a molar mass of  $M$  and molar gas constant  $R$ ,  $c_s$  is the so-called sticking constant, which takes on a value close to 1 for metals [19, 20].

The plasma arc pressure force is taken into account as follows [21]:

$$\mathbf{f}_{pl} = -p_{pl}(x, y)\mathbf{n}, \quad p_{pl}(x, y) = 2k_I I_a^2 \exp\left(-\frac{2}{R^2}((x-x_0)^2 + (y-y_0)^2)\right). \quad (8)$$

The radiation is modeled by the *Stefan-Boltzmann* equation:

$$s_{rad} = \sigma_B \varepsilon (T - T_0)^4, \quad (9)$$

where  $\sigma_B$  is Boltzmann constant,  $\varepsilon$  is material emissivity,  $T_0$  is ambient temperature.

The *Smoothed Particle Hydrodynamics (SPH)* method was used to solve this mathematical model and a series of numerical experiments were carried out to determine the basic regularities of the formation of deposited beads and the transfer of the filler material, the dependence of the geometrical characteristics of the deposited beads on the influence of the vapor pressure forces, the direction of the heat sources and the azimuthal angle of the heat sources. The variants of the electron-beam deposition process were analyzed at the location of the deposition velocity vector in the plane of the electron beams (Fig. 1, *a*) and perpendicular to this plane (Fig. 1, *b*).

The following geometrical characteristics of the simulated system and preliminary process parameters were used in the calculations (Table 1).

The austenitic chromium-nickel steel *04Cr18Ni10* was considered as a filler and a substrate material in the simulation (thermal physical characteristics are presented in Table 2).

Numerical realization was performed on a 2×300 sas 15k multiprocessor IBM computer (4xIntel Xeon E7520, 64 GB) using MPI multithreading capabilities of the *LAMMPS* package.

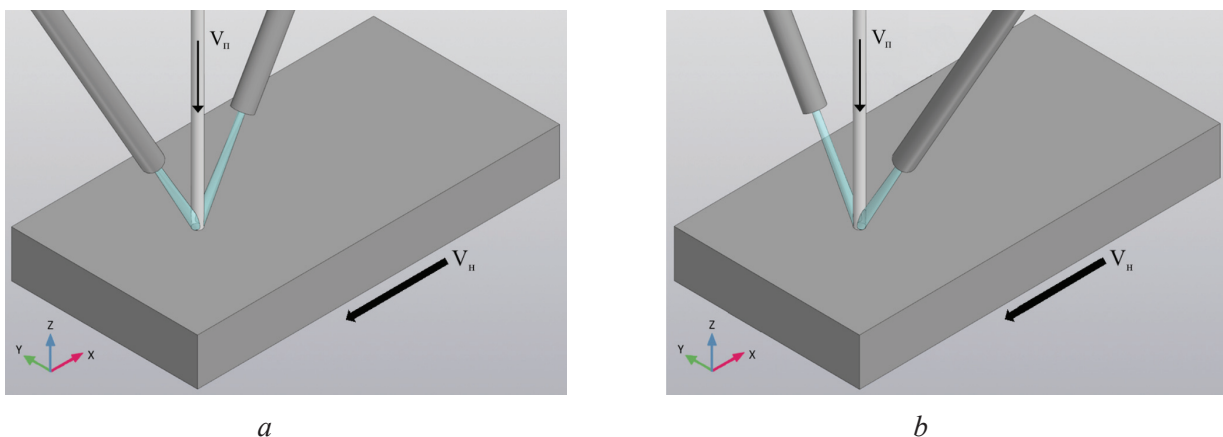


Fig. 1. Variants of the relative position of the deposition velocity vector and the action plane of the electron beams:

*a* – the deposition velocity vector lies in the action plane of the electron beams; *b* – the deposition velocity vector is perpendicular to the action plane of the electron beams

Table 1

## System characteristics

Characteristics	Designation	Dimension	Value
Substrate size	$L \times B \times H$	mm	20×10×3.5
Wire diameter	$d_w$	mm	1.2
Wire feed speed	$V_{wf}$	mm/sec	30
Substrate motion speed (deposition speed)	$V_s$	mm/sec	15
Diameter of heat sources (electron beams)	$D$	mm	1.5
Thermal power of each source	$Q$	W	350
Azimuthal angle of the heat sources action	$\alpha$	°	45/15

Table 2

## Thermal physical characteristics of 04Cr18Ni10 steel used in the calculation

Characteristics	Designation	Dimension	Value
Melting temperature	$T_{melt}$	K	1.800
Specific heat capacity	$C_p$	$J \cdot kg^{-1} \cdot K^{-1}$	710
Density	$\rho$	$kg \cdot m^{-3}$	7.680
Thermal conductivity	$\lambda$	$W \cdot m^{-1} \cdot K^{-1}$	26
Enthalpy of fusion	$H_f$	J/kg	276.000
Boiling Point	$T_{evp}$	K	3.133
Enthalpy of evaporation	$H_{evp}$	J/kg	351.000
Dynamic viscosity	$\mu$	Pa·s	0.007
Surface tension coefficient	$\sigma$	$N \cdot m^{-1}$	1.615
Temperature coefficient of surface tension	$\gamma = d\sigma/dT$	$N \cdot m^{-1} \cdot K^{-1}$	-0.00043

**Investigation of the influence of mutual positioning of the deposition velocity vector relative to the action plane of electron beams.** Figs. 2 and 3 show the results of numerical analysis of the deposition process of vertically fed wire material, fused by two symmetrically acting electron beams, without (a) and with (b) the forces of metal vapor pressure. Fig. 2 shows a variant in which the deposition velocity vector lies in the action plane of the electron beams, and Fig. 3 shows a variant in which the deposition velocity vector is perpendicular to the action plane of the electron beams.

The results testify that the geometric characteristics of the deposited beads significantly depend on the relative position of the deposition velocity vector relative to the action plane of the electron beams.

Without taking into account the vapor pressure forces, in both cases we observe the formation of fairly uniform rolls without significant distortion of the fusion line and the stream transfer of the filler material into the melt bath.

The vapor pressure force and its accounting has a significant impact on the results of numerical simulation of the formation of the welding pool and the hydrodynamic processes occurring in it, as it is known that the vapor pressure forces are the main driving force in the weld pool [22]. The mode of the filler material transfer also changes.

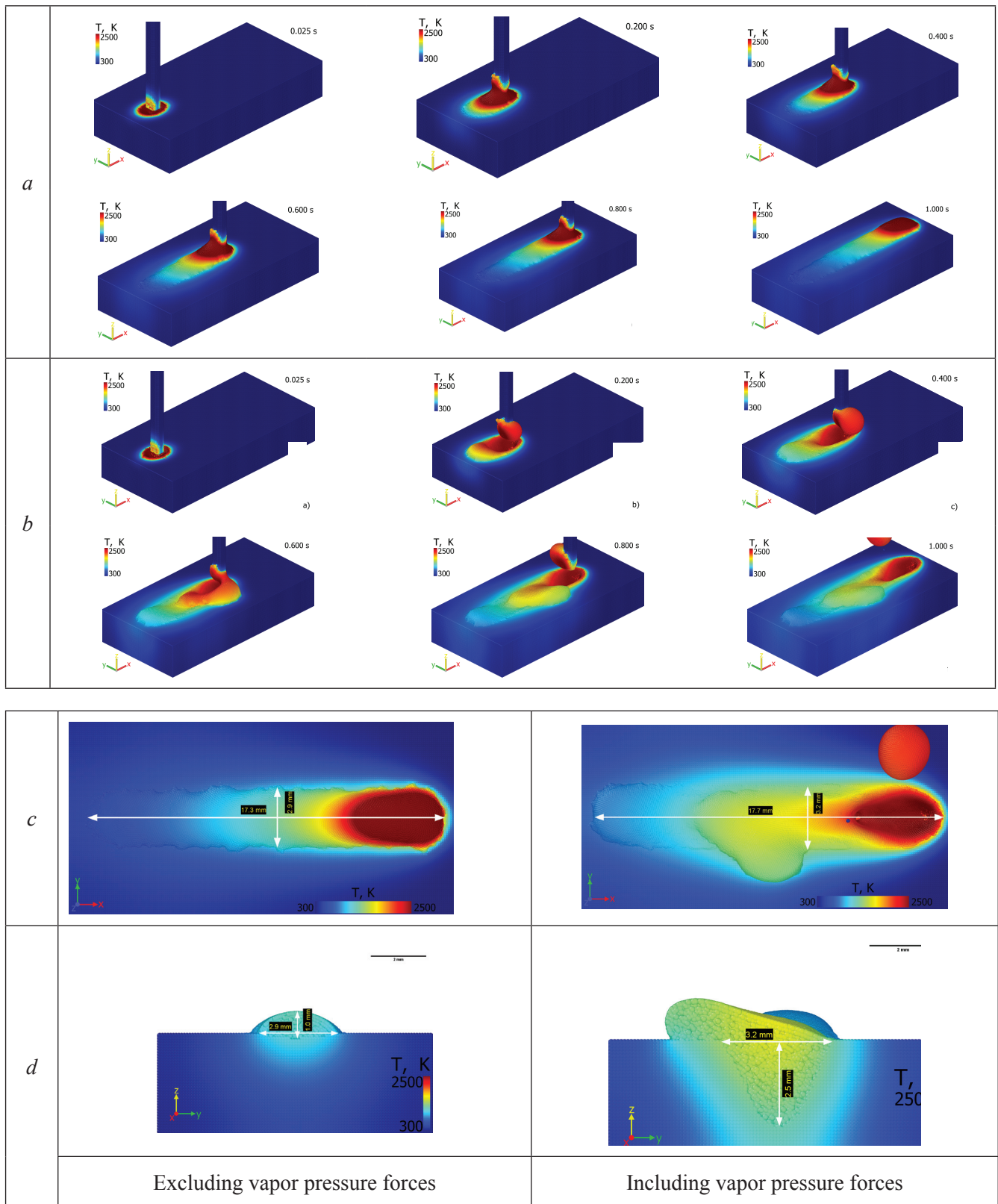


Fig. 2. The results of numerical calculation of the deposition process of vertically fed wire material melted by two symmetrically acting electron beams, for the variant in which the deposition velocity vector lies in the action plane of the electron beams:

*a* – fragments of the results of numerical analysis excluding metal vapor pressure; *b* – fragments of numerical analysis results including metal vapor pressure forces; *c* – geometric characteristics of the deposited beads; *d* – cross sections of fusion zones and geometry of the beads (power of each heat source is 350 W, azimuthal angle of each heat source is  $45^\circ$  to the vertical)

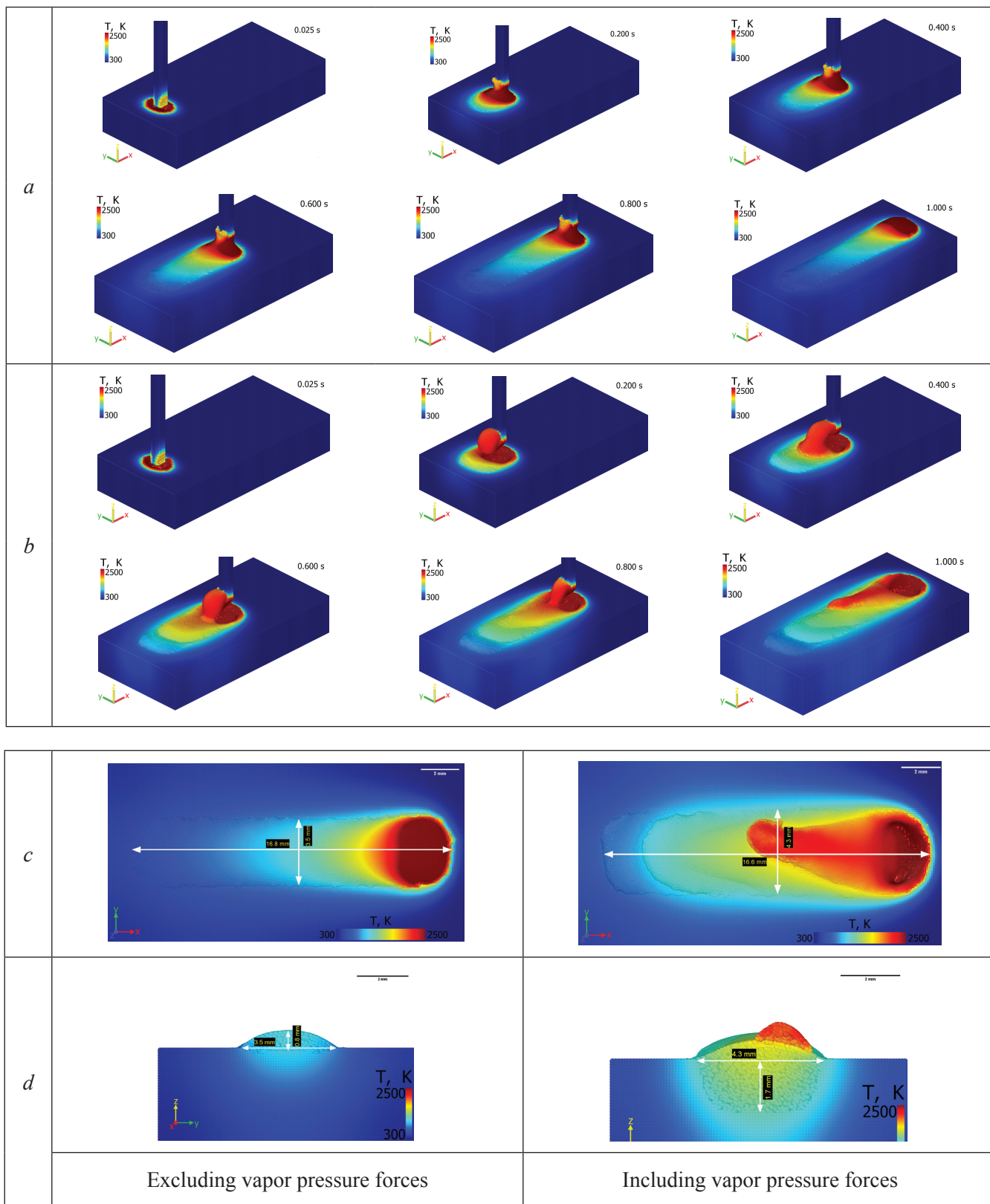


Fig. 3. Results of numerical calculation of the of the deposition process of a vertically fed wire material melted by two symmetrically acting electron beams, for the variant in which the deposition velocity vector is perpendicular to the plane of action of the electron beams:

*a* – fragments of the results of numerical analysis excluding metal vapor pressure; *b* – fragments of numerical analysis results including metal vapor pressure; *c* – geometric characteristics of the deposited beads; *d* – cross sections of fusion zones and geometry of the beads (power of each heat source is 350 W, azimuthal angle of each heat source is 45 ° to the vertical)

When the action of vapor pressure forces is taken into account, numerical calculations show a much greater depth of penetration of the base metal, the width of the deposited beads in this case increases by about 20 %. Under the action of vapor pressure forces in the liquid metal, a crater is formed and the metal is displaced to the periphery of the liquid weld pool. The crater has an elongated shape in the direction coinciding with the projection of the plane of action of electron beams. Changes in the ratio of forces acting on the weld pool and the formed filler material droplets lead to a transition to the coarse-droplet metal transfer.

Taking into account the vapor pressure forces, when the deposition velocity vector is located in the plane of the electron beam action, there is an asymmetry in the geometry of the deposited beads. This is due to the fact that the vapor pressure force vectors from the effects of thermal sources, being in the location plane of the deposition vector, limit the movement of the liquid metal in the longitudinal direction and displace it to the periphery of the deposited bead; with the direction of surges have a stochastic nature.

At the location of the deposition velocity vector perpendicular to the plane of action of electron beams, a more uniform geometry of the beads is observed, because the distribution of forces acting on the weld pool does not prevent the movement of the liquid metal into its tail part. In this case, there are no local surges outside of the deposited bead.

***Investigation of the effect of the azimuthal tilt angle of the electron beams.*** Figs. 4 and 5 show the results of numerical analysis of the deposition process of vertically fed wire material, fused by two symmetrically acting electron beams, at different azimuthal tilt angles of the electron beams.

The computational results show that as the azimuthal angle decreases, the projection area of electron beams on the substrate plane decreases, while the width of the active zone also decreases. This leads to an increase in the height of the deposited beads while the volume of the filler material is maintained. The energy density in the heating spot and the penetration ability of the electron beams also increases.

When the velocity vector is located in the plane of action of electron beams with a decrease in the azimuthal angle of each source, the depth of penetration increases and the height of the deposited bead increases. The width of the deposited beads remains practically unchanged.

Reducing the azimuthal angle has a positive effect on the uniformity of the deposited beads, eliminating the possibility of local surges to the periphery, while the entire incoming filler metal is involved in the formation of the bead and there is a fine-drop transfer of the filler material.

As the azimuthal angle of each source increases, the probability of surges to the periphery increases, due to the fact that the vapor pressure force vectors from the effects of thermal sources, located in the plane of the depositing vector limit the movement of the melt in the longitudinal direction and the more it is pushed to the periphery of the deposited bead, the closer the azimuthal angle of each source to the horizontal.

When the velocity vector is perpendicular to the plane of action of electron beams with a decrease in the azimuthal angle of action of each source, the width of the deposited beads decreases and the depth of substrate penetration and height of deposited beads increases.

## Results and discussion

Numerical experiments to determine the dependences of the geometric characteristics of the deposited beads on the influence of the vapor pressure forces, the direction of action of the heat sources and the azimuthal angle of the heat sources showed that consideration of the vapor pressure force has a significant impact on the results of numerical simulation of the formation of the weld pool and the hydrodynamic processes occurring in it, as well as on the transfer modes of the filler metal.

It was found that at the location of the deposition velocity vector perpendicular to the plane of action of electron beams, a more uniform geometry of the rolls is observed, because the distribution of forces acting on the weld pool does not prevent the movement of the liquid metal to its tail part. At the same time, increasing the azimuthal angle of action of heat sources increases the probability of surges to the periphery of the deposited bead, which is associated with the limitation of the melt movement in the longitudinal direction by the vapor pressure forces.

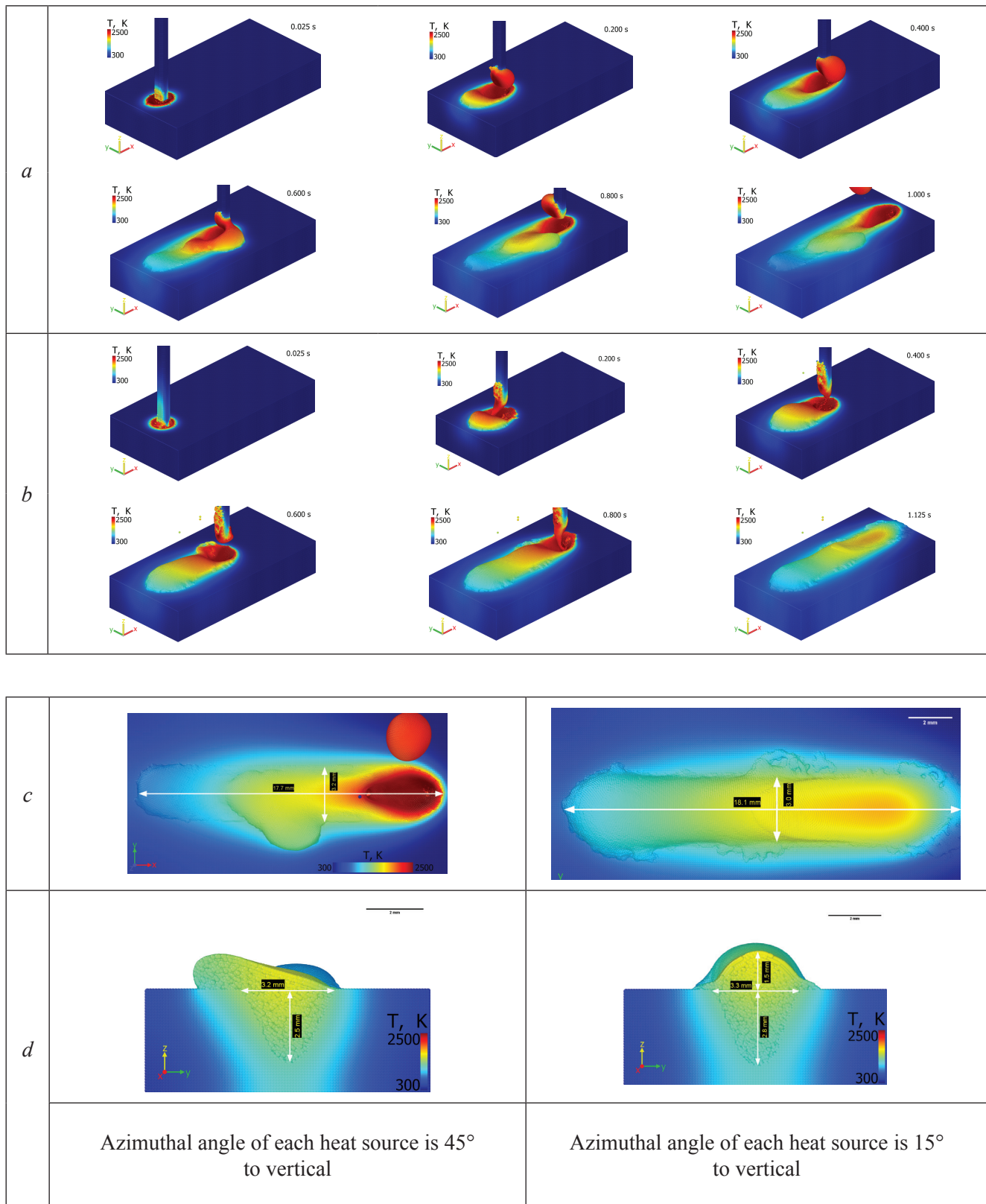


*Fig. 4.* Results of numerical calculation of the deposition process of a vertically fed wire material, melted by two symmetrically acting electron beams, for the variant in which the deposition velocity vector lies in the action plane of the electron beams:

*a* – fragments of the results of numerical analysis at an azimuthal angle of inclination of each electron beam 45° to the vertical; *b* – fragments of the results of numerical analysis at an azimuthal angle of inclination of each electron beam 15° to the vertical; *c* – geometric characteristics of the deposited bead; *d* – cross-sections of the penetration zones and geometry of the beads (power of each heat source is 350 W)

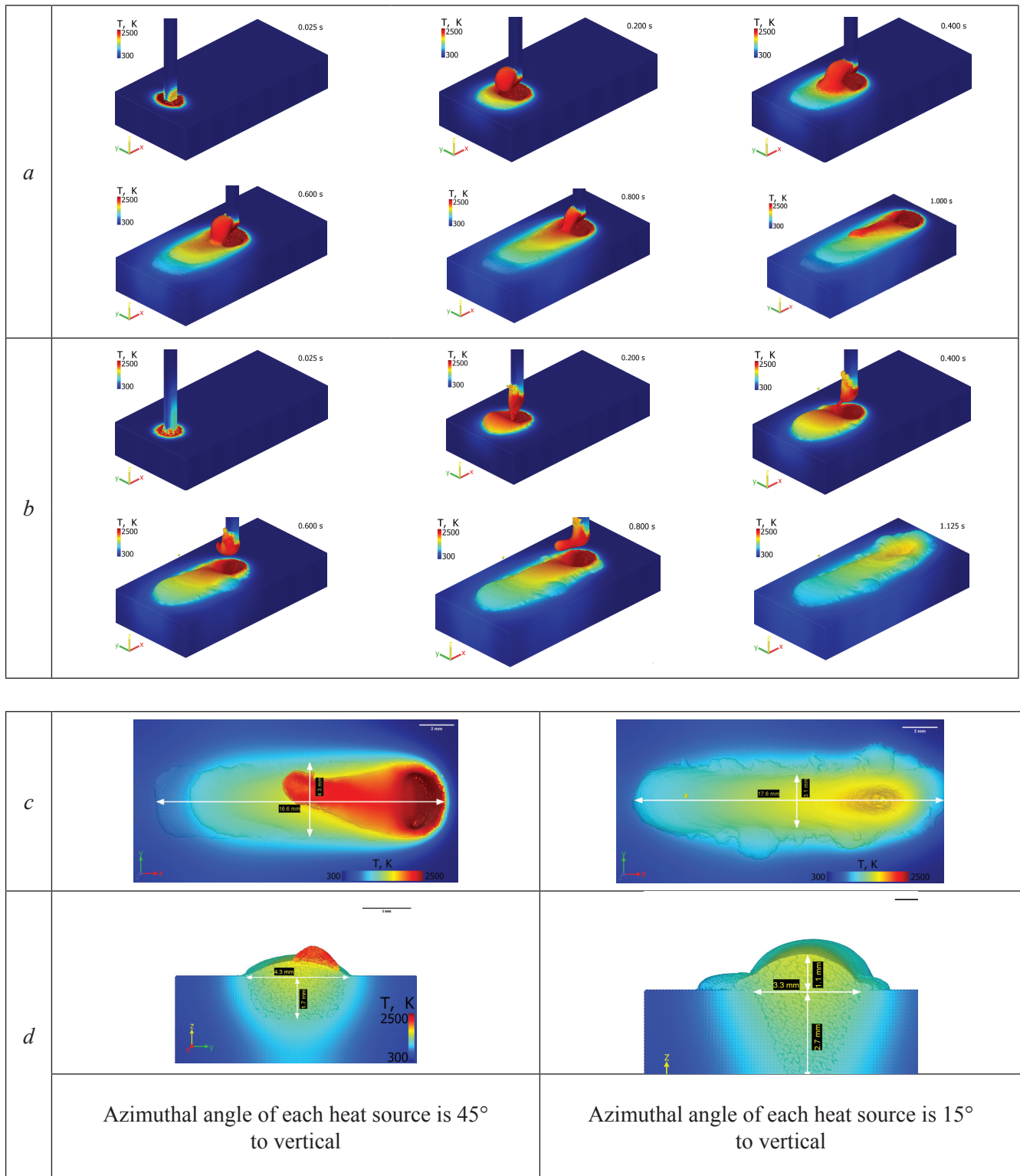


Fig. 5. Results of numerical calculation of the deposition process of a vertically fed wire material, melted by two symmetrically acting electron beams, for the variant in which the deposition velocity vector is perpendicular to the plane of action of the electron beams:

*a* – fragments of the results of numerical analysis at an azimuthal angle of inclination of each electron beam 45° to the vertical; *b* – fragments of the results of numerical analysis at an azimuthal angle of inclination of each electron beam 15° to the vertical; *c* – geometric characteristics of the deposited bead; *d* – cross-sections of the penetration zones and geometry of the beads (power of each heat source is 350 W)



## Conclusion

The results of numerical analysis of additive electron-beam deposition of wire material, melted by two symmetrically acting electron beams, confirmed the need to consider the influence of vapor pressure forces, due to the significant influence on the hydrodynamic processes in the weld pool, transfer modes of the filler material and, consequently, on the formation of deposited beads.

As a result of numerical experiment, the best formation of deposited beads is provided at a smaller azimuthal tilt angle of each electron beam to the vertical, in this case, there are minor distortions in the shape of the deposited beads from the location of the deposition velocity vector relative to the action plane of the electron beams, which also confirms the prospects for the developed technology for production parts with complex shapes.

The next stage of research will be verification and calibration of the mathematical model using experimental data, in order to ensure the possibility of predicting the deposition results and further optimization of the process.

## References

1. Taminger K.M., Hafley R.A. *Electron beam freeform fabrication (EBF<sup>3</sup>) for cost effective near-net shape manufacturing. NASA technical memorandum. NASA/TM-2006-214284* URL. Hampton, VA, National Aeronautics and Space Administration, Langley Research Center, 2006. Available at: <https://ntrs.nasa.gov/citations/20060009152> (accessed 23.06.2022).
2. Stecker S. *Electron beam layer manufacturing*. Patent US, no. 2016/0288244 A1, 2016.
3. Taminger K.M., Domack C.S., Zalameda J.N., Taminger B.L., Hafley R.A., Burke E.R. In-process thermal imaging of the electron beam freeform fabrication process. *Proceedings of SPIE – The International Society for Optical Engineering*, 2016, vol. 9861, p. 986102. DOI: 10.1117/12.2222439.
4. Fuchs J., Schneider C., Enzinger N. Wire-based additive manufacturing using an electron beam as heat source. *Welding in the World*, 2018, vol. 62, pp. 267–275. DOI: 10.1007/s40194-017-0537-7.
5. Gudenko A.V., Sliva A.P., Dragunov V.K., Shcherbakov A.V. Osobennosti formirovaniya izdelii metodom elektronno-luchevoi naplavki [Features of the formation of products by electron-beam surfacing]. *Svarochnoe proizvodstvo = Welding International*, 2018, no. 8, pp. 12–19. (In Russian).
6. Taminger K.M., Hafley R.A., Fahringer D.T., Martin R.E. Effect of surface treatments on electron beam freeform fabricated aluminum structures. *2004 International Solid Freeform Fabrication Symposium*, Austin, TX, 2004, pp. 460–470. DOI: 10.26153/tsw/7012.
7. AWS C7.1M/C7.1:2013. *Recommended practices for electron beam welding and allied processes*. American Welding Society, 2013. 150 p. ISBN 0-87171-721-2.
8. Bird R.K., Atherton T.S. *Effect of orientation on tensile properties of Inconel 718 block fabricated with electron beam freeform fabrication (EBF3). NASA Technical Memorandum. NASA/TM-2010-216719*. Hampton, VA, National Aeronautics and Space Administration, Langley Research Center, 2010. Available at: <https://ntrs.nasa.gov/citations/20100025706> (accessed 23.06.2022).
9. Wang L., Felicelli S.D., Coleman J., Johnson R., Taminger K.M.B., Lett R.L. Microstructure and mechanical properties of electron beam deposits of AISI 316L stainless steel. *Proceedings of the ASME 2011 International Mechanical Engineering Congress and Exposition. Vol. 3: Design and Manufacturing*, Denver, Colorado, USA, 2011, pp. 15–21. DOI: 10.1115/IMECE2011-62445.
10. Ivanchenko V.G., Ivasishin O.M., Semiatin S.L. Evaluation of evaporation losses during electron-beam melting of Ti-Al-V alloys. *Metallurgical and Materials Transactions B*, 2003, vol. 34 (6), pp. 911–915. DOI: 10.1007/s11663-003-0097-7.
11. Wang Y., Fu P., Guan Y., Lu Z., Wei Y. Research on modeling of heat source for electron beam welding fusion-solidification zone. *Chinese Journal of Aeronautics*, 2013, vol. 26 (1), pp. 217–223. DOI: 10.1016/j.cja.2012.12.023.
12. Chowdhury S., Nirsanametla Y., Muralidhar M. Studies on heat transfer analysis of Ti2AlNb electron beam welds using hybrid volumetric heat source. *Proceedings of the International Congress 2017 of the International Institute of Welding*, 07–09 December 2017, Chennai, India, 2017.
13. Trushnikov D., Perminov A., Belenkiy V., Permyakov G., Kartashov M., Matveev E., Dushina A., Schitsyn Y., Pang S., Karunakaran K.P. Modelling of heat and mass transfer for wire-based additive manufacturing using



electric arc and concentrated sources of energy. *International Journal of Engineering and Technology*, 2018, vol. 7, no. 4.38, pp. 741–747. DOI: 10.14419/ijet.v7i4.38.25777.

14. Mladenov G.M., Koleva E.G., Trushnikov D.N. Mathematical modelling for energy beam additive manufacturing. *Journal of Physics: Conference Series*, 2018, vol. 1089, art. 012001. DOI: 10.1088/1742-6596/1089/1/012001.

15. Trushnikov D.N., Permyakov G.L., Varushkin S.V., Davlyatshin R.V., Bayandin Y.V., Pang S. Improving the electron-beam additive manufacturing growth of components. *Russian Engineering Research*, 2021, vol. 41, no. 9, pp. 874–876. DOI: 10.3103/S1068798X21090276. Translated from *STIN*, 2021, no. 6, pp. 38–40.

16. Brackbill J., Kothe D. Dynamic modeling of the surface tension. *Proceedings of the Third Microgravity Fluid Physics Conference*, Cleveland, OH, NASA Lewis Research Center, 1996, pp. 693–698.

17. Anisimov S.I., Khokhlov V.A. *Instabilities in laser-matter interaction*. Boca Raton, FL, CRC Press, 1995. 141 p. ISBN 0-8493-8660-8.

18. Cho J.-H., Farson D.F., Milewski J.O., Hollis K.J. Weld pool flows during initial stages of keyhole formation in laser welding. *Journal of Physics D: Applied Physics*, 2009, vol. 42, no. 17. DOI: 10.1088/0022-3727/42/17/175502.

19. Khairallah S.A., Anderson A.T., Rubenchik A., King W.E. Laser powder-bed fusion additive manufacturing: Physics of complex melt flow and formation mechanisms of pores, spatter and denudation zones. *Acta Materialia*, 2016, vol. 108 (16), pp. 36–45. DOI: 10.1016/j.actamat.2016.02.014.

20. Leitz K.-H., Grohs C., Singer P., Tabernig B., Plankensteiner A., Kestler H., Sigl L.S. Fundamental analysis of the influence of powder characteristics in Selective Laser Melting of molybdenum based on a multi-physical simulation model. *International Journal of Refractory Metals and Hard Materials*, 2018, vol. 72, pp. 1–8. DOI: 10.1016/j.ijrmhm.2017.11.034.

21. Strakhova E.A., Erofeev V.A., Sudnik V.A. Fiziko-matematicheskoe modelirovanie protsessa shirokosloinoi naplavki s poperechnymi kolebaniyami plazmotrona [Physical-mathematical modeling of wide-layer surfacing with transverse oscillations of plasma torch]. *Svarka i diagnostika = Welding and Diagnostics*, 2009, no. 3, pp. 32–38. (In Russian).

22. Semak V., Matsunawa A. The role of recoil pressure in energy balance during laser materials processing. *Journal of Physics D: Applied Physics*, 1997, vol. 30, no. 18, pp. 2541–2552.

## Conflicts of Interest

The authors declare no conflict of interest.

© 2022 The Authors. Published by Novosibirsk State Technical University. This is an open access article under the CC BY license (<http://creativecommons.org/licenses/by/4.0/>).